Research Article Adv. Mat. Lett. 2013, 4(12), 905-909 ADVANCED MATERIALS Letters

www.amlett.com, www.amlett.org, DOI: 10.5185/amlett.2013.5472 Published online by the VBRI press in 2013

Synthesis of porous titania and its application to dye-sensitized solar cells

Ammar Elsanousi[1,2*], Kamal Khalifa Taha[1], Nazar Elamin[1]

[1]*College of Applied and Industrial Sciences, University of Bahri, Khartoum, Sudan*
[2]*School of Material Science and Engineering, Hebei University of Technology, Tianjin 300130, P. R. China*

[*]Corresponding author. E-mail: aelsanousi@hotmail.com

Received: 02 May 2013, Revised: 04 July 2013 and Accepted: 07 July 2013

ABSTRACT

Nanocrystalline porous titania with rutile and anatase bi-phase structure has been fabricated by the sol-gel method without the introduction of any surfactant, using tetrabutile titanate as precursor. The porous material was integrated as an electrode in a dye-sensitized solar cell as an electrode and its photoelectrical parameters were measured. Experimental measurements showed that the cell exhibits higher values of short-circuit current density and overall conversion efficiency compared to P25 (typical commercial titania powder) cells. The overall conversion efficiency of both samples was calculated to be 2.81 and 1.57 for the prepared and commercial (P-25) sample respectively. This drastic increase in the conversion efficiency of the prepared sample was attributed to its high surface area and porous structure, allowing more sensitizer dye to be chemically anchored in the electrode and, as a consequence, improved the light harvesting drastically. These results indicate that it is possible to achieve commendable conversion efficiencies using porous bi-phase titania.

Keywords: Titanium dioxide; nanoparticles; DSSC; sol-gel, P-25.

Ammar Elsanousi is an Assistant Professor of Physics at Bahri University, Khartoum, Sudan. He has received his Ph. D. degree from Huazhong University, China in 2009, and has worked as researcher at Hebie University of Technology, Tianjin, China 2013. His main research interest is synthesis, properties and applications of Nanomaterials for photovoltaic solar cells and clean energy. He has published more than 20 research articles in international journals.

Kamal Khalifa Taha is an Associate Professor of Physical Chemistry and has worked as Dean College of Applied and Industrial Sciences at the University of Bahri, Khartoum, Sudan 2011-2013. His main research interest is synthesis of advanced materials for environmental chemistry. He has published many articles in journals of international repute.

Nazar Elamin is an Assistant Professor of Physics at Bahri University, Khartoum, Sudan. He has received his Ph. D. degree from Bahri University, Sudan in 2012. His main research interest is Synthesis and Applications of Nanomaterials for water purification and environmental science. He has many publications in the field of environmental science.

Introduction

Solar energy is a clean energy that can be directly converted to electricity in photovoltaic cells without pollution, noise, or mechanical parts. The idea to convert solar light directly to electricity is not new, where solar-electricity conversion cells have been produced since several decades ago, however the conventional solar cell is expensive for large-scale production **[1, 2]**.

In the past decade, a new solar cell design, based on nanostructured materials has been advanced. This cell was first reported by Gratzel and co-workers in 1991 and is called the dye-sensitized solar cell (DSSC) **[3-7]**. DSSCs are extremely promising because they are made of low-cost materials and do not need elaborate apparatus to manufacture, while still providing a reasonable energy-conversion efficiency. In addition, the materials used in the DSSC are environment friendly **[8]**.The main difference between the DSSC and the conventional silicon based solar cells is that in the DSSC the functional element, which is responsible for light absorption (the dye), is separated from the charge carrier transport **[9-12]**. The dye absorbs the energy from the sunlight, and thereby undergoes photo-excitation to an excited state. The excited electron is then injected into the conduction band of the semiconductor (TiO_2), leaving the dye in an oxidized state. The electron is then transferred by the semiconductor to the conducting glass and through the external load back to the counter

electrode where it reduces the oxidized species of the electrolyte. At the same time the oxidized dye accepts an electron from the reduced species of the electrolyte and returns to its ground state, and the circuit is closed **[13-16]**.

Recently, considerable research efforts have concentrated on the factors influencing the overall conversion efficiency of a DSSC. M. Gratzel **[17]** reported that porous titania (TiO_2) electrodes with high surface area allows absorption of a larger amount of dye, resulting in better cell performance. N-G. Park *et.al* **[18]** suggested that increasing the particle packing density as well as increasing the surface area by producing a densely packed film of nanosized particles will improve the photo-conversion efficiency of the DSSC. On the other hand, smaller pore size seems to obstruct the penetration of the dye molecule inward the film and reduce the amount of the adsorbed dye **[19]**. The photon-to-current conversion efficiency is related to many parameters that include light harvesting for photons, quantum yield for electron injection from excited sensitizer into the conduction band of the semiconductor, electron collection efficiency and nanocyrstalline film thickness **[20]**. Therefore, the precise balance of particle size, pore size, porosity, effective area and thickness of the film is important to achieve optimum cell performance.

A wide variety of methods have been developed for the synthesis of porous TiO_2 nanoparticles so far such as spray pyrolysis deposition (SPD) technique **[21]**, sol–gel **[22-24]** and hydrothermal method **[25]**.

In this article, we present the production of porous TiO_2 nanoparticles, synthesized without using any surfactant and their application to dye-sensitized solar cell. Measurements showed that the porous nanoparticles cell exhibits higher performance compared to DSSCs assembled by standard commercial (Degussa, P-25) TiO_2 nanoparticles, indicating that DSSCs based on such a porous structure shows a possibility of an improved performance with increased efficiency.

Experimental

Materials

All chemicals were used as received, without any further purification processes; Tetrabutile titanate (TBOT, 98%, Beijing LYS Chemicals Co. Ltd, China), cis-di(thiocyanato) bis (2,2´-bipyridyl-4,4´-dicarboxylate) ruthenium (II) (N719 dye, Sigma Aldrich, USA). Ethanol and hydrochloric acid were of analytical reagent grade and were purchased from Shanghai Reagent Co. Ltd, China.

Preparation of TiO_2 nanoparticles

Porous titania nanoparticles were prepared without using any surfactant (will be denoted hereafter as N-TiO_2) by the sol-gel technique as follows; 23 ml of tetrabutile titanate (4Ti (C_4H_9O) was added to 23ml of ethanol, the resulting solution was stirred for 15 minutes at room temperature. A mixed solution of 23 ml of ethanol and 18g of 4.4M HCl aqueous solution was added dropwise to the former solution under vigorous stirring at room temperature for 30 minutes. The resulting mixture was held for hydrolysis in an incubator at 40°C for 4 days. The obtained gel was then milled and annealed at 600° C for 2 hours with heating and cooling rates of 20°C/min.

Characterization

The crystal phase composition of the sample was characterized by powder X-ray diffraction (XRD; D/max-RB) using a Bruker D8 diffractometer with Cu kα radiation (λ=0.154178 nm). To determine the average crystallite size, peak broadening analysis was applied to anatase and rutile diffraction peaks using Scherrer's equation. The morphology and grain size of the titania nanoparticles were examined by scanning electron microscopy (SEM, JEOL JSM-6700F). The powder samples were ultrasonically dispersed in ethanol and transferred onto carbon-coated copper grids for the transmission electron microscopy (TEM, JEOL, JEM-2010F) analysis.

DSSC assembly and measurement

The prepared porous titania nanoparticles photoelectrode was immersed for 24 h in a solution of the sensitizer: cis-di(thiocyanato) bis (2,2´-bipyridyl-4,4´-dicarboxylate) ruthenium (II) (abbreviated as N-719 dye) dissolved in absolute ethanol. The counter electrode was transparent conducting oxide (TCO) glass on which 340 nm thick layer of Pt was deposited by sputtering. An adhesive tape was placed between the two electrodes, in order to control the electrolyte film thickness and to avoid short-circuiting of the cell. A drop of the redox electrolyte containing 0.3 M LiI and 0.03 M I_2 in propylene carbonate, was introduced between the clamped electrodes by the capillary force to finalize the assembly of the DSSC. The photocurrent (I) and photovoltage (V) of the cell were measured with an active area of 0.08 cm^2 using simulated sunlight at AM-1.5 produced by Oriel 91192 solar simulator. The solar energy-to-electricity conversion efficiency (η) was determined by the following equation;

$$\eta = \frac{J_{SC} \times V_{OC} \times FF}{I_0} \times 100\,(\%) \qquad (1)$$

Where, J_{SC} is the short-circuit photocurrent, V_{OC} is the open-circuit photovoltage, FF is the fill factor of the cell and I_0 is the intensity of the incident light. For comparison, commercial titania nanoparticles (Degussa, P-25 with a primary particle size of 21 nm) film was also assembled into DSSC with the same film thickness and its photoelectrical parameters were also measured.

Results and discussion

Fig. 1 shows the X-ray diffraction patterns of the porous TiO_2 nanoparticles prepared without surfactants compared to P-25 commercial nanoparticles powder. The diffraction peaks of the prepared sample (N-TiO_2) correspond to crystalline titanium dioxide with a mixed phase of anatase and rutile, while the pattern of the commercial nanopowder (P-25) shows a pure anatase phase structure. The phase composition of N-TiO_2 sample and commercial P-25 was calculated from the following equation: **[22]**.

$$X_R = 1 - \left[1 + 1.26\left(\frac{I_R}{I_A}\right)\right]^{-1} \qquad (2)$$

where X_R is the weight fraction of rutile in the mixture, and I_R and I_A are the peak intensities of the rutile (110) and anatase (101) diffractions, respectively and the results are listed in **Table 1**.

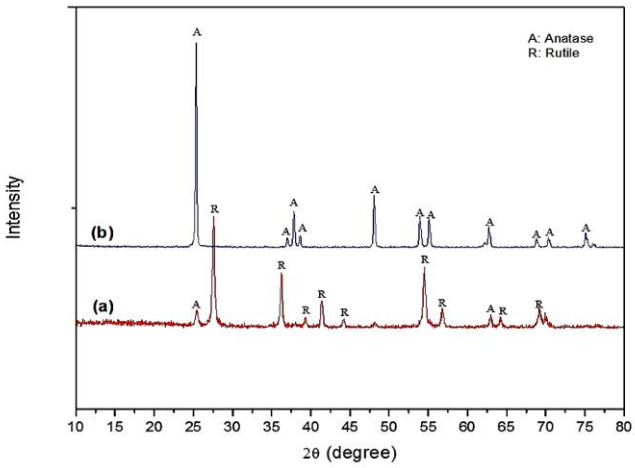

Fig. 1. X-ray diffraction patterns of: (a) prepared TiO_2 nanoparticles and (b) commercial P-25 nanopowder.

Table 1. Average particle sizes of samples calculated by Scherrer's equation.

Sample	Average particle size (nm)	Crystal structure	
		Phase	Rutile (%)
N-TiO_2	28	anatase / rutile	90
P-25	21	anatase	0

The average particle size of crystalline TiO_2 was roughly estimated by calculation from the width of the XRD peaks using the Scherrer equation:

$$D = \frac{k\,\lambda}{\beta \cos\theta} \qquad (3)$$

Where k is a constant (0.94), λ is the XRD wavelength, β is the corrected half-width of the strongest diffraction peak and θ is the diffraction angle. The average particle size of the powders is also summarized in **Table 1**. From this table, the prepared sample (N-TiO_2) exhibits an average particle size of about 28 nm, composed of bi-phase structure with a dominant rutile phase (90%), while the commercial (P-25) shows pure anatase phase with an average particle size of 21nm.

Fig. 2 shows the SEM images of TiO_2 nanoparticles prepared without the addition of surfactant. The sample shows a porous structure of aggregated nanoparticles with a large particle size distribution in the range between 20-50nm. This broadened particle size distribution can be attributed to the bi-phase structure of anatase and rutile crystals existing in the sample.

In order to confirm the morphological structure and identity of the resulting product, TEM analysis was performed for the sample. The nanoparticle size and particle size distribution shows a good agreement with the SEM analysis as can be seen from **Fig. 3**.

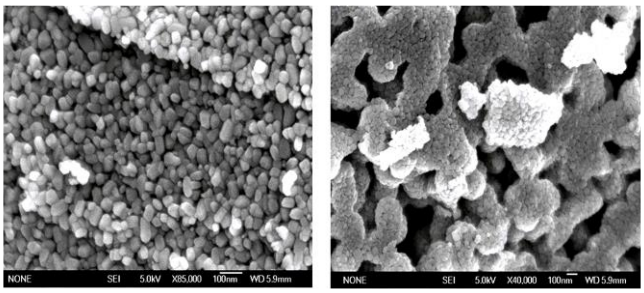

Fig. 2. SEM images of TiO_2 nanoparticles prepared without surfactant.

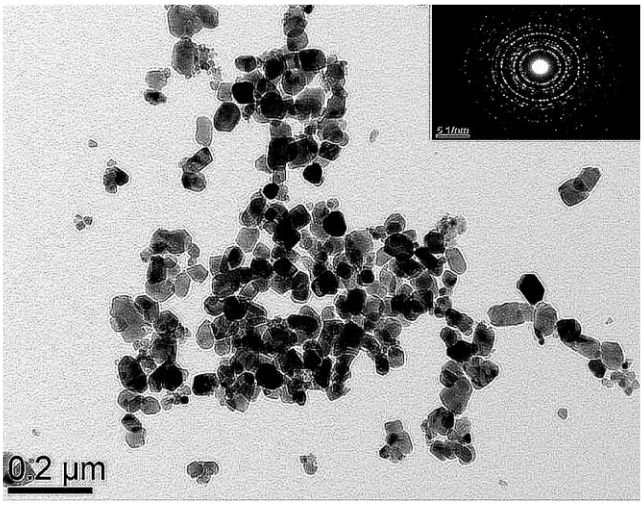

Fig. 3. TEM micrographs of TiO_2 nanoparticles prepared without surfactants (inset is SAED pattern).

The selected area electron diffraction (SAED) analysis shows a polycrystalline structure, as indicated by the ring pattern in the inset of **Fig. 3**. The lattice spacing (d) was calculated for the prepared porous nanoparticles and was found to have a value of about 0.325 nm corresponding to the rutile phase (110) according to the pfd card number [21-1276]. These results match well with the phase composition calculations made by equation 2. Although the phase composition calculated from equation 2 shows a bi-phase structure, but the calculation of the phase composition from the SAED pattern can only show the composition of the dominant phase, which is 90% rutile phase.

The prepared (N-TiO_2) nanoparticles and commercial (P-25) nanopowder were assembled into DSSCs and their photoelectrical parameters were measured. **Fig. 4** shows the photocurrent-voltage curves of these samples. The overall conversion efficiency of the samples was calculated to be 2.81 and 1.57 for (N-TiO_2) and (P-25) respectively. The photoelectrical parameters of both samples are summarized in **Table 2**.

Generally, the results show very low short-circuit current density (J_{SC}) and overall conversion efficiency (η) for both samples compared to other reported data, due to some technical aspects concerning the type of electrolyte and Pt coated counter electrode quality. However, the results provide a good overview for comparison.

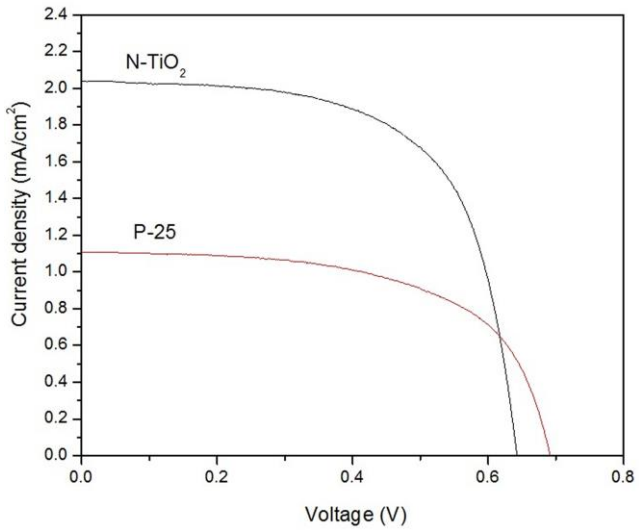

Fig. 4. Photocurrent-voltage curves of DSSC based on TiO_2 nanoparticles prepared without the introduction of surfactant compared to standard commercial P-25 TiO_2.

Table 2. Photoelectrical parameters of the cells prepared with different nanopowders.

Sample	J_{SC} (mA/cm²)	V_{OC} (Volt)	FF (%)	η (%)
N-TiO_2	2.036	0.642	0.64	2.80
P-25	1.110	0.691	0.60	1.57

Observations showed that the DSSC assembled with TiO_2 nanoparticles prepared without the introduction of surfactant (N-TiO_2) presented much higher values of short-circuit current density and overall conversion efficiency in comparison to the commercial standard (P-25) sample. This increase in the efficiency of the DSSC can be ascribed to the existence of rutile phase in the prepared sample, where it has been reported by Zhang *et.al* **[26]** that the presence of rutile crystals extends the life of electron-hole pairs by forming sites that trap electron and thus delaying the recombination process. The drastic increase in the short-circuit current density for the (N-TiO_2) sample can be attributed to its high surface area and porous structure, which allows more sensitizer dye to be chemically anchored in the electrode and, as a consequence, the light harvesting is drastically improved. In addition, the porous structure allows the electrolyte to penetrate the film all the way to the back-contact making the semiconductor/electrolyte interface essentially three-dimensional. To confirm this, the absorption spectra of the sensitized TiO_2 films were measured by UV–vis spectroscopy and the spectra are shown in **Fig. 5**. From this figure it was observed that the absorbance intensity measured for the (N-TiO_2) sample is much higher than that of (P-25) (for the same film thickness) specially at the absorption peaks of N 719 dye at the wavelengths of 535 and 398 nm, which maximizes the photon absorption and thus increases the photocurrent and consequently enhances the overall conversion efficiency. For the standard (P-25) sample, it was observed that the absorbance intensity is relatively low due to the compact layer of the film caused by the uniform particle size distribution for this sample, resulting in a low dye adsorption and hence lower short-circuit current density. On the other hand, this compactness in the electrode provides an inter-connected structure, which enhances the electron transport through the nanoparticles to the back contact, and thus resulting in higher open-circuit voltage and fill factor.

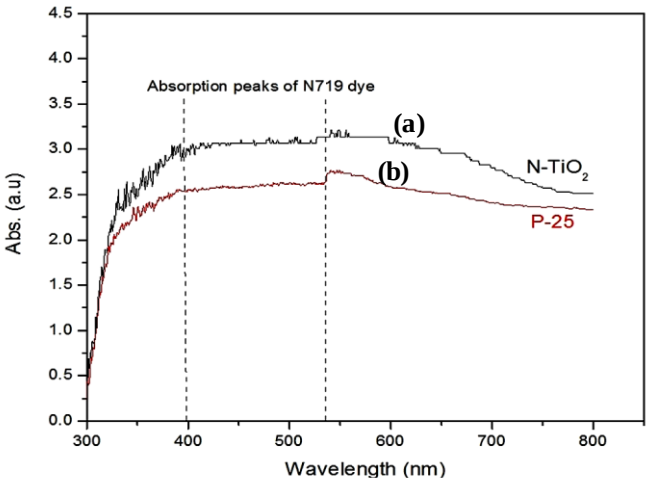

Fig. 5. UV–vis spectra of N719 dye adsorbed on TiO_2 nanoparticle samples: (a) prepared nanoparticles without surfactant and (b) commercial TiO_2 nanoparticles (P-25).

Conclusion

Porous titania with bi-phase structure of rutile and anatase was fabricated by sol-gel without using any surfactant. The porous titania film was integrate as an electrode in a dye-sensitized solar cell and its photoelectrical parameters were measured. Measurements showed that the DSSC assembled with TiO_2 nanoparticles prepared without the introduction of surfactant (N-TiO_2) presents much higher values of short-circuit current density and overall conversion efficiency compared to commercial (P-25) nanoparticles cells. The overall conversion efficiency of both samples was calculated to be 2.81 and 1.57 for (N-TiO_2) and (P-25) respectively. This drastic increase in the conversion efficiency of the prepared (N-TiO_2) sample was attributed to its high surface area and porous structure, which allows more sensitizer dye to be adsorbed in the electrode and thus increases the harvested light.

Reference

1. Pode, R., *Adv. Mat. Lett.* 2011, 2(1), 3. **DOI**: 10.5185/amlett.2010.12186
2. Thankalekshmi, R.R.; Dixit, S.; Rastogi, A. C., *Adv. Mat. Lett.* 2013, 4(1), 9. **DOI**: 10.5185/amlett.2013.icnano.137
3. O'Regan, B.; Gratzel, M., *Nature*, **1991**, 353, 737. **DOI**: 10.1038/353737a0
4. Chappel, S.; Zaban, A.; *Sol. Energy Mater. Sol. Cells*, **2002**, 71, 141. **DOI**: 10.1016/S0927-0248(01)00050-2
5. Rani, S; Suri, P; Shishodia, P.K.; Mehra, R.M., *Sol. Energy Mater. Sol. Cells*, **2008**, 92, 1639. **DOI**: 10.1016/j.solmat.2008.07.015
6. Lira-Cantu, M.; Krebs, F.C.; *Sol. Energy Mater. Sol. Cells*, **2006**, 90, 2076. **DOI**: 10.1016/j.solmat.2006.02.007

7. Ito, S.; Murakami, T.N.; Comte, P.; Liska, P; Gratzel, C.; Nazeeruddin, M.K.; Gratzel, M.; *Thin Solid Films*, **2008**, 516, 4613. **DOI**: 10.1016/j.tsf.2007.05.090
8. B. Li, L. Wang, B. Kang, P. Wang, Y. Qiu, *Sol. Energy Mater. Sol. Cell*., 90 (2006) 549.
9. Gratzel, M., *Current Applied Physics*, **2006**, 6S1, e2. **DOI**: 10.1016/j.cap.2006.01.002
10. Schmidt-Mende, L; Gratzel, M., *Thin Solid Films*, **2006**, 500, 296. **DOI**: 10.1016/j.tsf.2005.11.020
11. Gratzel, M.; J. Photochem. Photobiol. C: *Photochem. Rev*., **2003**, 4, 145. **DOI**: 10.1016/S1389-5567(03)00026-1
12. Gratzel, M.; *J. Photochem. Photobiol. A: Chem.*, **2004**, 164, 3. **DOI**: 10.1016/j.jphotochem.2004.02.023
13. Gratzel, M.; *Prog. Photovoltaics*, **2000**, 8, 171. **DOI**: 10.1002/(SICI)1099-159X(200001/02)8:1<171::AID-PIP300>3.0.CO;2-U
14. Mills, A.; Le Hunte, S., *J. Photochem. Photobiol. A*, **1997**, 108, 1. **DOI**: 10.1016/S1010-6030(97)00118-4
15. Li, Y.; Hagen, J.; Schaffrath, W.; Otschik, P.; Haarer, D., *Sol. Energy Mater. Sol. Cells*, **1999**, 56, 167. **DOI**: 10.1016/S0927-0248(98)00157-3
16. Hart, J.N.; Menzies, D.; Cheng, Y-B.; Simon, G.P.; Spiccia, L., *Sol. Energy Mater. Sol. Cells*, **2007**, 91, 6. **DOI**: 10.1016/j.solmat.2006.06.059
17. Gratzel, M., *Curr. Opin. Colloid Interface Sci*., **1999**, 4, 314. **DOI:** 10.1016/S1359-0294(99)90013-4
18. Park, N-G.; Van de Lagemaat, J.; Frank, A. J., *J. Phys. Chem. B*, **2000**, 104, 8989. **DOI**: 10.1021/jp994365l
19. Mor, G.K.; Shankar, K.; Paulose, M.; Varghese, O.K.; Grimes, C.A., *Nano Lett.*, **2005**, 5, 191. **DOI**: 10.1021/nl048301k
20. Adachi, M.; Jiu, J.; Isoda S., *Current Nanoscience*, **2007**, 3, 285.
21. Okuya, M.; Nakade, K.; Kaneko, S., *Sol. Energy Mater. & Sol. Cells*, **2002**, 70, 425. **DOI**: 10.1016/S0927-0248(01)00033-2
22. Jung, H.S.; Shin, H.; Kim, J.R.; Kim, J.Y.; Hong, K.S.; Lee, J.K., *Langmuir*, **2004**, 20, 11732. **DOI**: 10.1021/la048425c
23. Han, D.; Li, Y.; Jia, W., *Adv. Mat. Lett.* **2010**, 1(3), 188. **DOI**: 10.5185/amlett.2010.7137
24. Yuan, Z.; Zhang, J.; Li, B.; Li, J., *Thin Solid Films*, **2007**, 515, 7091. **DOI**: 10.1016/j.tsf.2007.02.101
25. Hsiao, P.-T.; Lu, M.-D.; Tung, Y.-L; Teng, H., *J. Phys. Chem. C*, **2010**, 114, 15625. **DOI**: 10.1021/jp1061013
26. Li, H.; Zhang, W.; Pan, W., *J. Am. Ceram. Soc.* **2011**, 94, 3184. **DOI**: 10.1111/j.1551-2916.2011.04748.x

